

The histology of two female Early Cretaceous birds

Jingmai K. O'CONNOR¹ WANG Min¹ ZHENG Xiao-Ting^{2,3} WANG Xiao-Li^{2,3}
ZHOU Zhong-He¹

(1 Key Laboratory of Vertebrate Evolution and Human Origins of Chinese Academy of Sciences, Institute of Vertebrate Paleontology and Paleoanthropology, Chinese Academy of Sciences Beijing 100044 jingmai@ivpp.ac.cn)

(2 Institute of Geology and Palaeontology, Linyi University Linyi, Shandong 276000)

(3 Shandong Tianyu Museum of Nature Pingyi, Shandong 273300)

Abstract We conduct histological analysis of two sexually mature fossil birds from the Lower Cretaceous Jehol Group referable to *Jeholornis* sp. and *Enantiornithes* indet. Histology confirms that in these lineages of basal birds, sexual maturity was achieved before skeletal maturity. The samples reveal structural differences from previously described relevant specimens, indicating that the ontogenetic changes in bone tissue that occur in Mesozoic birds are more complicated than previously recognized. The female specimen of *Jeholornis* sectioned here is more vascularized than previously described specimens, with both reticular and longitudinal canals. The enantiornithine bone tissue is most similar to that reported for the Early Cretaceous *Concornis*, primarily formed by parallel-fibered bone but more vascularized than other reported adult enantiornithine specimens. The bone shows a distinct decrease in the rate of bone deposition, inferred to represent the onset of sexual maturity.

Key words Mesozoic, histology, *Jeholornis*, *Enantiornithes*, Jehol Biota

1 Introduction

The Lower Cretaceous Jehol Group is arguably the most important geologic unit in the world for understanding the early evolution of birds (Zhou et al., 2003; Zhou, 2004; Benton et al., 2008). The Jehol Biota includes the oldest and most basal pygostylian clades (*Confuciusornithiformes*, *Sapeornithiformes*), the earliest appearance of the avian beak (*Confuciusornis*, *Archaeorhynchus*), the earliest record of the dominant Cretaceous clade of birds (*Enantiornithes*), and the earliest record of the lineage that includes living birds (*Ornithuromorpha*) (O'Connor et al., 2011; Zhou and Zhang, 2006). The Jehol Biota also includes *Jeholornis* (Zhou and Zhang, 2002), a long bony-tailed bird that has been suggested to be the most basal known avian taxon — if *Archaeopteryx* is removed from *Aves* (Xu et al., 2011). Despite the great potential to learn about the growth rate and developmental strategy of extinct organisms through histological analysis (Chinsamy et al., 1995, 2013; Chinsamy and Elzanowski, 2001; Erickson et al., 2009; Schweitzer et al., 2005) and the large number of

available specimens (Chang et al., 2003), a relatively limited number of specimens of birds and dinosaurs have been sampled from the Lower Cretaceous Jehol Group (Chinsamy et al., 2013; Erickson et al., 2009; Zhang et al., 1998). This is due in part to exaggerated misconceptions regarding the destructive nature of this process, and in part due to the poor preservation (or even absence) of the bone in many specimens, which is particularly an issue among earlier discoveries (e.g. *Boluochia*, *Chaoyangia*, *Cathayornis*) (Hou and Zhang, 1993; Zhou, 1995; Zhou et al., 1992). As a result, the few histological analyses that have been published often present conflicting data, such as reports that *Confuciusornis* completed growth within a year, like modern birds, vs. newer studies that suggest more prolonged growth (de Ricqlès et al., 2003; Zhang et al., 1998), and growth in Early Cretaceous birds remains poorly understood.

Here we report on the histology of one recently described specimen of *Jeholornis* sp. (STM 2-51) and one specimen of *Enantiornithes* indet. (STM 29-8) (Zheng et al., 2013). These specimens are considered female based on the interpretation of circular structures preserved in the body cavity as mature ovarian follicles, and their histology has been previously briefly discussed with regard to the formation of medullary bone (Zheng et al., 2013), an ephemeral type of bone tissue found in ovulating female birds (Miller and Bowman, 1981), and reported in some dinosaurs and basal birds (Schweitzer et al., 2005; Chinsamy et al., 2013). Unfortunately, specialized medullary bone tissue could not be identified in either specimen and the histology was not described in detail (Zheng et al., 2013). Due to the limited information available regarding basal bird histology, these samples deserve further discussion, thus here we present a full description of the histology of these two Early Cretaceous birds.

The histology of *Jeholornis* has only been reported from two specimens (Erickson et al., 2009). No histological analyses on enantiornithines from the Jehol Group have been published although one specimen of *Concornis* from the Early Cretaceous of Spain (Cambra-Moo et al., 2006) and four Late Cretaceous specimens have been studied (Chinsamy et al., 1994, 1995; Chinsamy and Elzanowski, 2001; Wang et al., in press). Because of the phylogenetic and temporal distribution between the few sampled specimens, the enantiornithine growth strategy remains enigmatic; however, what is known reveals a very different strategy from that of living birds (Chinsamy et al., 1995). Here we provide a complete description of the morphological details of the histological samples from these two fossil bird specimens and compare the results to previous reports for these taxa.

Institutional abbreviations IVPP, Institute of Vertebrate Paleontology and Paleoanthropology, Chinese Academy of Sciences, Beijing, China; LH, Las Hoyas Collection, Museo de Cuenca, Cuenca, Spain; MACN, Museo Argentino de Ciencias Naturales “Bernardino Rivadavia”, Buenos Aires, Argentina; PVL, Paleontología de Vertebrados Lillo, Universidad Nacional de Tucúman (National University of Tucúman), Tucúman, Argentina; STM, Shandong Tianyu Museum of Nature, Pingyi, China; ZPAL, Zoological Institute of Paleobiology, Polish Academy of Sciences, Warsaw, Poland.

2 Methods

Jeholornis STM 2-51 is a large specimen, with a humeral length of 118.3 mm and a femoral length of 88 mm. Using the equations by Liu et al. (2012), body mass is estimated from the humerus to be 688.4 g. Enantiornithine STM 29-8 is a medium sized specimen, with a humeral length of 44.7 mm and a femoral length of 40.2 mm; body mass is estimated to be 146.8 g (Liu et al., 2012). Two bone samples were taken from each of the specimens, as close to midshaft as preservation allowed: the ulna and femur were sampled in STM 2-51 and the humerus and femur were sampled in STM 29-8 (Fig. 1). The samples were taken using a micro-saw and were embedded in EXAKT Technovit 7200 one-component resin and allowed to dry for 24 hours. The samples were then cut and polished until the desired optical contrast was reached. The samples were viewed under normal and polarized light using a Leica DM-RX polarizing microscope. Measurements were taken with the computer software ImageJ 1.43r. Histological terminology is mainly sensu de Ricqlès (1976) and Chinsamy-Turan (2005). We follow Erickson et al. (2009) and consider channels as an indicator of the extent of vascularization.

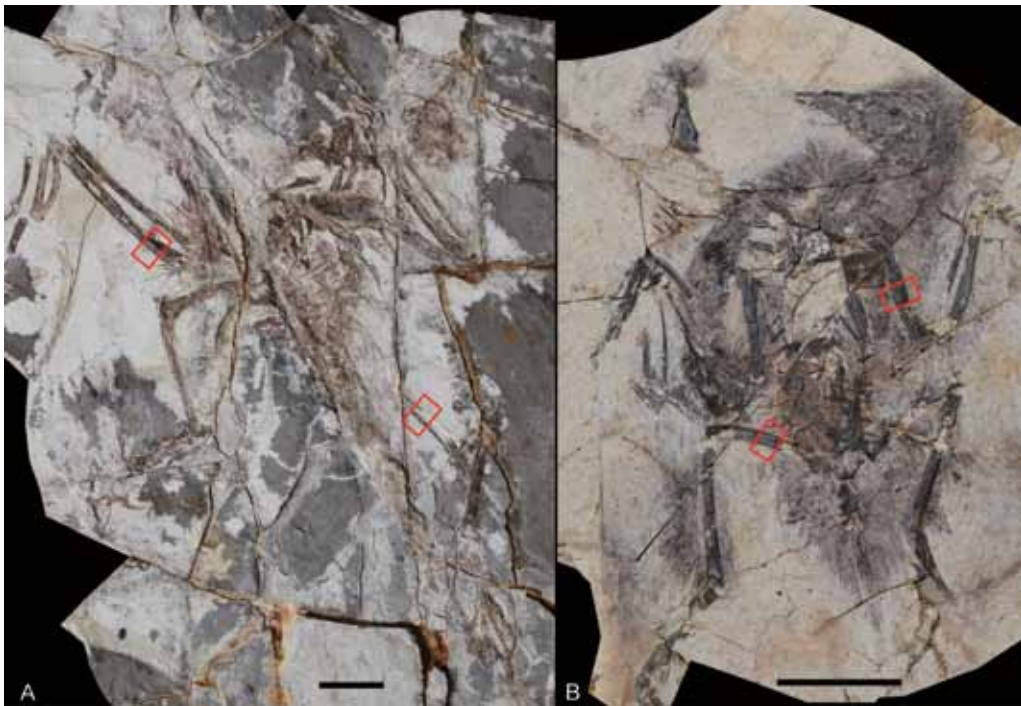


Fig. 1 Photographs of *Jeholornis* sp. STM 2-51 (A) and *Enantiornithes* indet. STM 29-8 (B) Boxes indicate where the histological sections were sampled; the upper boxes indicate where the forelimb elements were sampled, ulna (A) and humerus (B) respectively; the lower boxes mark where the femora were sectioned. Scale bars equal 4 cm

3 Results

3.1 *Jeholornis* sp. STM 2-51

Ulna The thin section of the ulna (Fig. 2A) is stratified into three distinct regions (or layers): an inner poorly vascularized region of avascular endosteally derived lamellated bone tissue (inner circumferential layer, ICL or medullary lining bone) with collagen fibers and osteocyte lacunae arranged nearly parallel; a thick middle region of more woven-textured bone tissue with plump, haphazardly organized osteocyte lacunae; and an outer region (outer circumferential layer, OCL) of avascular parallel-fibered bone tissue with parallel osteocyte lacunae that are flatter than those in the ICL (Fig. 2A, 3B). The ICL forms one-third the cortical thickness. The ICL and middle region are separated by an uneven tide line, clearly visible under polarized light, representing where resorption occurred during medullary expansion before the ICL was deposited during growth reversal (Fig. 3A)(Chinsamy-Turan, 2005). The middle region of the compacta is richly vascularized; there is a predominance of longitudinally oriented vascular canals although there is also reticular vascularization (not reported in previous specimens of *Jeholornis*), and primary osteons are abundant (Fig. 2A, 3A). A few isolated secondary osteons are also visible indicating some remodeling of the bone tissue occurred (Fig. 2A). Osteons are most abundant closer to the ICL and vascularization becomes predominantly longitudinal closer to the OCL so that the boundary with the more parallel fibered OCL is not distinct, interpreted as a gradual decrease in growth rate. A double line of arrested growth (double LAG)(Castanet et al., 1993) is regarded as the boundary between the middle region and the avascular parallel-fibered OCL (Fig. 2A, 3B). At least two more LAGs occur close to the periosteal surface of the bone; these are not considered rest lines because they are not tightly layered although they are close and evenly spaced. The cortical thickness increased by 8% between the double LAG and the next LAG in the OCL, but only by 2%-3% between subsequent LAGs (Fig. 3B). The periosteal surface is smooth rather than undulating indicating it was completely ossified (Chinsamy and Elzanowski, 2001). The endosteal or medullary surface is broken but moderately well preserved; still, no medullary bone can be identified. In some places, perpendicular cracks are visible intruding the inner circumferential layer from the medullary cavity (Fig. 3A).

Femur The thin section of the femur (Fig. 2B) also reveals three regions in the bone compacta. The inner region of endosteally derived lamellated bone tissue (ICL) is poorly preserved and potentially diagenetically altered although faint osteocyte lacunae are still visible. A majority of the compacta forms a thick middle region of more woven-textured bone tissue with plump, haphazardly organized osteocyte lacunae (Fig. 3C). This is surrounded by an outer layer (OCL) of avascular, more parallel fibered bone tissue with osteocyte lacunae that are flatter and arranged in parallel (Fig. 3D). The ICL is proportionately thinner compared to the ulna, forming only 20% of the cortical thickness. The middle region of the femur compacta

preserves a greater degree of reticular vascularization than the ulna, although canals are still predominantly longitudinal. Relatively fewer primary osteons are visible compared to the ulna, as evidenced by the lack of centripetal infilling of lamellated bone around the blood vessels, and no secondary osteons are observed (Fig. 2B). Primary osteons are mostly concentrated in one region, and occur up until the boundary with the OCL (Fig. 2B, 3C), unlike the ulna section where they are more interiorly restricted. A similar condition was previously reported for *Jeholornis*, although whether this also matches the thickest part of the compacta (Erickson et al., 2009) cannot be determined due to poor preservation in STM 2-51. The different growth rates around the circumference of the section suggest the bone was changing shape (remodeling) during the time of deposition (Chinsamy-Turan, 2005). The middle layer of bone loses its woven texture gradually towards the OCL. A LAG occurs roughly near the boundary with the outer region (Fig. 2B, 3D). A second LAG occurs near the smooth periosteal surface,



Fig. 2 Histology sections of *Jeholornis* sp. STM 2-51

A. ulna (area indicated by red box enlarged under polarized light in 3A); B. femur (area indicated by red box enlarged under polarized light in 3C)

Abbreviations: ICL. inner circumferential layer; ML. middle layer; OCL. outer circumferential layer. The compacta (i.e., compact bone wall) is made up of three distinct regions: 1) an inner region of endosteally derived lamellated bone tissue; 2) a middle region of more woven-textured bone tissue with reticular and longitudinal canals; and 3) an outer region of more parallel-fibered bone tissue marked by lines of arrested growth (LAG). White arrows indicate LAGs; open black arrows indicate the tide line marking the furthest extent of endosteal resorption, below which lies the inner circumferential layer (ICL); black and white arrows indicate primary osteons. Scale bars equal 100 μm

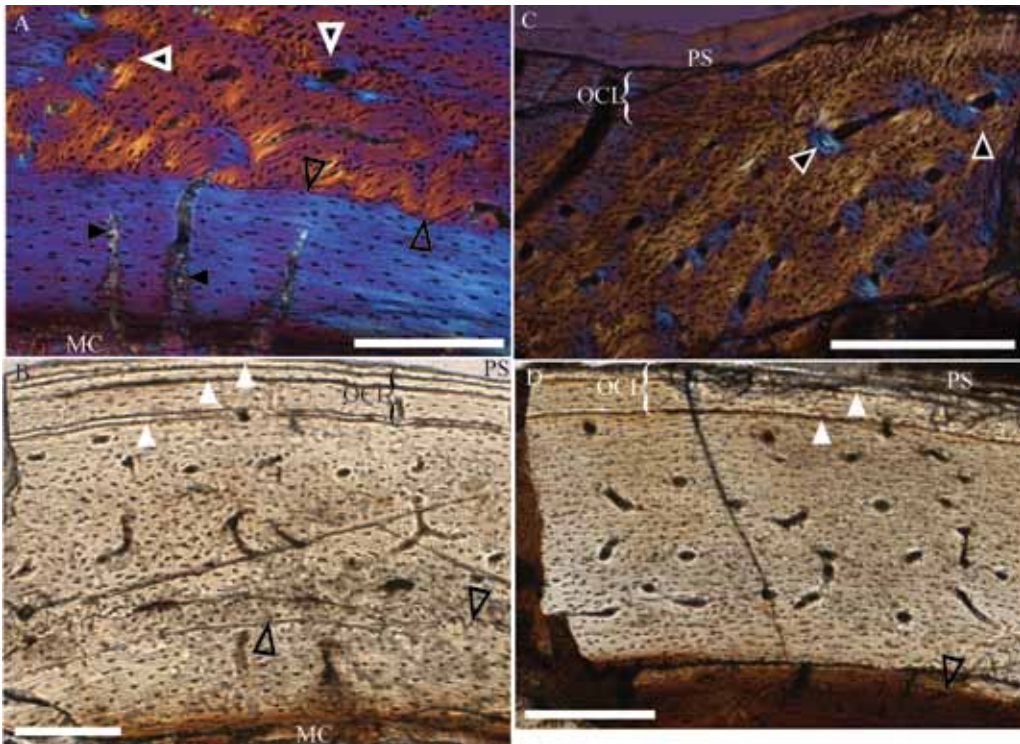


Fig. 3 Details of *Jeholornis* STM 2-51 histology

A. ulna under polarized light showing tide line between the endosteally derived lamellated bone and the more woven-textured bone that forms the middle layer; B. complete transverse cross section of the ulnar cortex showing three distinct layers: an inner layer of endosteally derived lamellated bone, a thick layer of woven-textured bone, and an outer layer of parallel-fibered bone; C. femur under polarized light showing region of bone with concentrated primary osteons; D. complete transverse cross section of the femoral compact bone wall showing three distinct layers, as in the ulna. White arrows indicate lines of arrest growth; open black arrows indicate the tide line and upper margin of the inner circumferential layer (ICL); black and white arrows indicate primary osteons; black arrows indicate cracks. All scale bars equal 50 μm

Abbreviations: MC. medullary cavity; OCL. outer circumferential layer; PS. periosteal surface

separated from the first LAG by a 6% increase in cortical thickness (Fig. 2B). The inner surface of the medullary cavity is broken and poorly preserved but no medullary bone appears to be present.

3.2 Enantiornithine STM 29-8

Humerus The bone compacta of the enantiornithine humerus is more difficult to interpret due to the lesser quality of preservation compared to *Jeholornis* STM 2-51 and observed variations around the circumference of the section. However, as in the Early Cretaceous Spanish enantiornithine *Concornis* (Cambra-Moo et al., 2006), three regions can be discerned: an inner avascular region of endosteally derived lamellated bone tissue with osteocyte lacunae arranged in parallel (ICL); a middle region of more vascularized bone tissue with plump and more haphazardly organized osteocyte lacunae; and a thick poorly

vascularized outer region (OCL) of parallel-fibered bone tissue with osteocyte lacunae that are flatter and arranged in parallel (Fig. 4A). The ICL is separated from the middle region by an uneven tide line, representing the furthest extent of medullary expansion, and varies from 6%-46% the cortical thickness (Fig. 4A, 5A). As in *Concornis*, extensions of the endosteal bone tissue can be observed penetrating the deeper cortex in some areas (Cambra-Moo et al., 2006). The middle region of the compacta is not as richly vascularized as in *Jeholornis*, and vascularization is entirely longitudinal; fewer primary osteons are present and these are entirely concentrated in a single area where the bone tissue is strongly woven. Secondary osteons are far more numerous compared to *Jeholornis* (Fig. 2) and are also especially concentrated in one area of the bone wall, near where the ICL is thickest; the large amount of remodeling may suggest this was the site of a muscle attachment (Fig. 4A). Similar to *Jeholornis* STM 2-51, within the middle region the primary osteons are concentrated closer to the ICL with fewer osteons and simple primary vascular canals towards the periosteal surface. The boundary with the OCL is not distinct; rather the osteocyte lacunae become increasingly flatter and more organized, suggesting a gradual slowing of growth. Furthermore, the thickness of the two layers are inversely related to each other indicating the bone was changing shape as it grew (Fig. 4A). An annulus, clearly visible under polarized light (Fig. 5A), followed by a LAG is found near the transition between the OCL and the middle region; its position varies from near the midpoint to closer to the periosteal surface (Fig. 4A). Although vascularization is atypical of the OCL (Chinsamy-Turan, 2005), there are more than a few simple blood vessels in the OCL of STM 29-8, all located in the thickest part of the OCL where the LAG and annulus occur closer to the middle of the compacta (Fig. 4A). The outer region of the OCL is poorly preserved and it cannot be determined if additional LAGs were present although the periosteal surface is smooth indicating it was completely ossified. Faint canaliculi are visible extending from some of the osteocyte lacunae in the middle region (Fig. 5B). The medullary surface is broken and no medullary bone can be identified.

Femur Interpretations of the thin section of the enantiornithine femur (Fig. 4B) are also obscured by poor preservation; the section is not complete in most places and some variation around the circumference is apparent. The femoral compacta is not clearly stratified although three regions can be distinguished. The compacta is divided into a thin, avascular inner layer of endosteally derived lamellated bone tissue (ICL); a thin middle region of parallel-fibered bone that grades from plump, haphazardly organized osteocyte lacunae into a thick upper region of parallel-fibered bone tissue with flatter osteocyte lacunae arranged in parallel (OCL; Fig. 4B). The inner region is not well preserved; it is separated from the middle region by a tide line (Fig. 5D). The bone tissue in the middle layer is poorly vascularized with entirely longitudinal canals and only one or two isolated primary and secondary osteons located in the inner half of the middle region, where the osteocyte lacunae are also more haphazardly arranged (Fig. 4B). As bone deposition continued it apparently slowed gradually and only simple primary vascular canals are present closer to the boundary with the OCL. The contact between the middle and

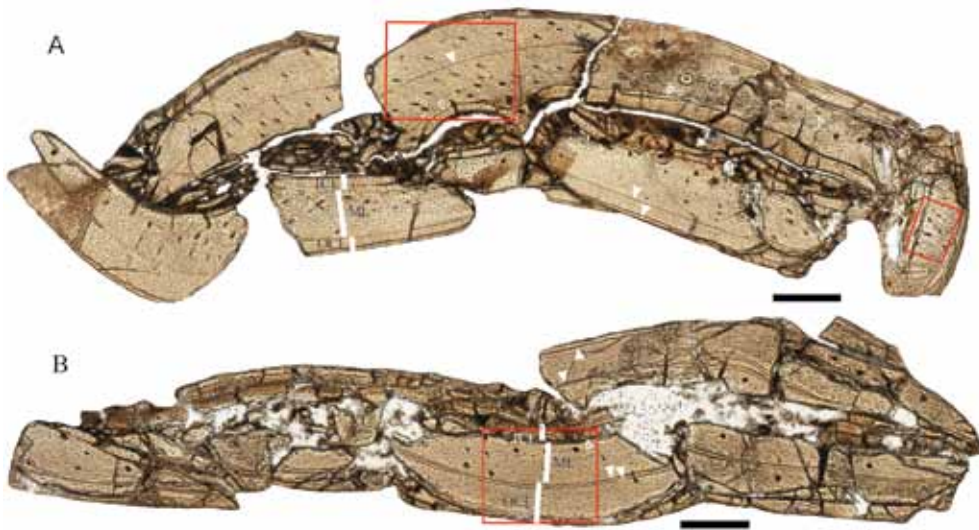


Fig. 4 Histology sections of *Enantiornithes* indet. STM 29-8

A. humerus (area indicated by larger red box enlarged under polarized light in 5A; area indicated by small red box enlarged in 5C, showing densely packed primary osteons), note the large cluster of secondary osteons in the upper right of the section; B. femur (area indicated by red box enlarged under polarized light in 5D). The compacta is made up of three distinct regions: 1) an inner region of endosteally derived lamellated bone tissue; 2) a middle region of more vascularized parallel-fibered bone; and 3) an outer region of avascular parallel-fibered bone tissue marked by lines of arrested growth. Note how the thickness of both the ICL and OCL vary around the section, especially in the humerus (A). For abbreviations see Fig. 2 caption. White arrows indicate lines of arrest growth; open white arrows indicate the tide line of the furthest extent of endosteal resorption, below which lies the inner circumferential layer (ICL) of endosteally derived lamellated bone tissue

Scale bars equal 100 μ m

upper regions is indistinct; a double LAG is situated at the transition, which may mark the onset of sexual maturity (Fig. 4B, 5D). The OCL forms approximately 50% of the cortical thickness; two-three isolated blood vessels are present, far fewer than observed in the humeral section. Although the periosteal surface was clearly smooth and fully ossified, the outermost compacta is not well preserved; potentially another LAG may have been present close to the outer surface. The medullary cavity is poorly preserved and no medullary bone is present (Fig. 4B).

4 Discussion

Understanding growth patterns from histological studies on basal birds is complicated by data that suggests that basal birds are incomparable to other studied groups (Chinsamy et al., 1995). Features indicative of skeletal maturity such as an ICL and OCL (Ponton et al., 2004) are not necessarily correlated in basal birds. Furthermore, basal birds display unique bone textures and combinations indicative of complex growth strategies that vary between clades. With the limited number of samples, interpretations remain inconclusive and strongly reinforce the need

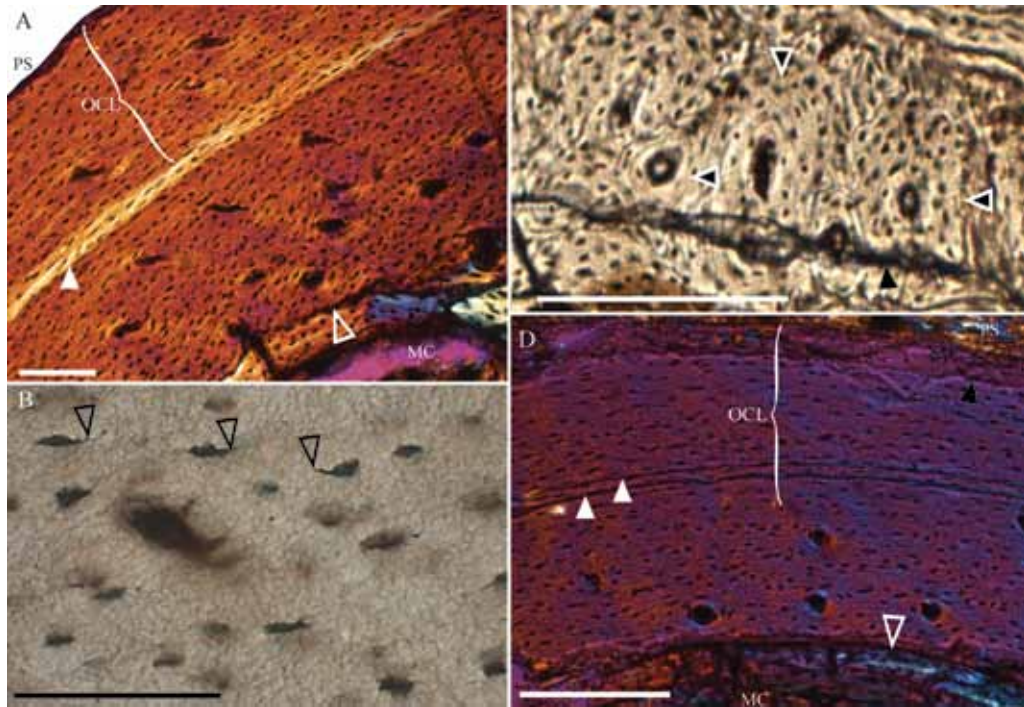


Fig. 5 Details of *Enantiornithes* indet. STM 29-8 histology

A. humerus under polarized light showing the annulus near the transition from vascular to avascular parallel-fibered bone; B. close up of the canaliculi visible around some osteocyte lacunae in the humerus; C. close up of primary osteons concentrated in one region of the humerus; D. femur under polarized light showing double LAG, marking inferred onset of sexual maturity. White arrows indicate lines of arrest growth; open white arrows indicate the tide line of the furthest extent of endosteal resorption, below which lies the inner circumferential layer (ICL) of endosteally derived lamellated bone tissue; black and white arrows indicate primary osteons; black arrows indicate cracks; open black arrows indicate canaliculi. For abbreviations see

Fig. 3 caption. All scale bars equal 50 μ m

for additional analysis. However, we discuss these new samples, compare with other specimens, and discuss potential interpretations based on the currently available data.

4.1 *Jeholornis* bone histology

The long bone compacta of *Jeholornis* STM 2-51, as revealed by sections from the ulna and femur, consists primarily of a thick ICL of endosteally derived lamellated bone with well organized collagen fibers, a thick middle region of vascularized woven textured bone, and a thinner OCL of primarily avascular parallel-fibered bone marked by several LAGs. The femur differs from the humerus in that the middle layer of bone tissue is less woven with fewer primary osteons suggesting that growth of the forelimb was faster than that of the hindlimb (Bennett, 2008). The bone compacta of STM 2-51 reveals some differences from previously sampled specimens (Erickson et al., 2009). Only the femur was sectioned in the previous study and thus comparison is limited to this element. STM 2-51 shows both longitudinal and

reticular oriented canals, whereas Erickson et al. (2009) only reported longitudinal canals. A LAG is reported in IVPP V 13353, the larger of the two specimens studied by Erickson et al. (2009). This LAG is located much closer to the medullary cavity, whereas in STM 2-51 the LAG is situated close to the boundary of the OCL. Furthermore, a tide line was not reported by Erickson et al. (2009), which may suggest additional LAGs were lost when bone was remodeled in STM 2-51 and thus an even older age for this specimen. Alternatively, Gao et al. (2012) consider that V 13353 preserves an ICL (separated by a tide line) interrupted by a LAG. However, we suggest that the LAG identified by Erickson et al. (2009) in V 13353 may actually be a tide line marking the boundary of the ICL and the furthest extent of medullary resorption (no LAG present), in which case this specimen is still interpreted as younger than STM 2-51.

Both the holotype of *Jeholornis prima* IVPP V 13274 and the referred specimen V 13353 that were sampled by Erickson et al. (2009) are smaller than STM 2-51 (Table 1). We estimate their body masses to be 601.2 and 285.4 g respectively (Liu et al., 2012). The difference in size is likely due to the older age and greater degree of somatic maturity at time of death in STM 2-51, which is consistent with histological data; the well formed ICL and limited amount of growth observed in the OCL between LAGs indicate STM 2-51 had reached sexual maturity (Chinsamy-Turan, 2005; Chinsamy et al., 1994) yet the absence of lamellar bone tissue forming the outermost compacta (a true OCL) may suggest the individual had not achieved skeletal maturity. STM 2-51 preserves bone tissue indicative of more rapid growth than that of V 13274 and V 13353, which may suggest a phase of rapid growth later in ontogeny. Erickson et al. (2009) used the samples from V 13274 and V 13353 to suggest basal birds required two to three years to reach skeletal maturity. The results of this study may suggest that V 13274 and V 13353 were subadults and that these basal birds required more than three years to reach skeletal maturity. Size differences could also potentially be explained through species specific growth trends or sexual dimorphism, although testing these competing hypotheses would require more histological data and a taxonomic investigation of known specimens. The bone histology of STM 2-51 is similar to that of *Rahonavis*, a controversial Late Cretaceous maniraptoran that is considered by some to be a long-tailed bird less derived than *Jeholornis* (Forster et al., 1998). The compacta is also formed by three distinct regions with a double LAG marking the lower boundary of the OCL in *Rahonavis* thin-sections, but in this taxon the ICL is thinner, the OCL is thicker, and the middle layer is fibrolamellar (Chinsamy and Elzanowski, 2001).

Table 1 Body mass estimates for sampled *Jehol* specimens

Taxon	Collection number	Length (mm)	Estimated mass (g)
<i>Jeholornis prima</i>	IVPP V 13274	110.5 (humerus)	601.2
	IVPP V 13353	71.9 (humerus)	285.4
<i>Jeholornis</i> sp.	STM 2-51	118.3 (humerus)	688.4
Enantiornithine sp.	STM 29-8	44.7 (humerus)	146.8
Enantiornithine sp.	MACN-S-01	93.5 (femur)	1805.5

4.2 Enantiornithine bone histology

The compacta of the humerus and femur of enantiornithine STM 29-8 reveal three layers of bone tissue: a distinct ICL of endosteally derived lamellated bone and a thin middle layer of more vascularized parallel-fibered bone that grades into an OCL of parallel-fibered bone with flat and organized osteocyte lacunae. Despite the diversity of the enantiornithine clade, only five other specimens have been sampled for comparison: an embryonic specimen of *Gobipteryx* (ZPAL MgR-/90) from the Late Cretaceous of Mongolia (Chinsamy and Elzanowski, 2001); *Parvavis* (IVPP V 18586), the first Late Cretaceous specimen from China (Wang et al., in press); a referred adult/subadult specimen of *Concornis* (LH 21006) from the Early Cretaceous of Spain (Cambra-Moo et al., 2006); and two isolated adult femora (PVL-4273 and MACN-S-01) from the Late Cretaceous of Argentina (Chinsamy et al., 1995). Although these specimens sample much of the ontogenetic spectrum, they are widely separated temporally, geographically, and or phylogenetically, obscuring attempts to understand enantiornithine growth strategies.

The morphology of the bone tissue in STM 29-8 most strongly resembles the histology observed in *Concornis* LH 21006, the only other published Early Cretaceous sample (Cambra-Moo et al., 2006), although comparison is slightly complicated by the fact that the sample in *Concornis* was taken from the tarsometatarsus, which tends to show greater degrees of remodeling compared to long bones and thus is not an ideal element for analysis. Still, both specimens preserve three histological layers with primary and secondary osteons in the middle layer. In contrast, the bone compacta of the Late Cretaceous *Parvavis* and the two from the Late Cretaceous Lecho Formation specimens (femora, PVL-4273 and MACN-S-01), is formed entirely by avascular parallel-fibered bone (Chinsamy et al., 1995; Wang et al., in press). The femora show two size classes of osteocyte lacunae, one much larger than the other with well-developed canaliculi; these are primarily limited to the inner half of the middle region of the bone and may have compensated for the absence of vascularization (Chinsamy et al., 1995). Only the smaller size class of osteocyte lacunae is present in STM 29-8 and *Concornis* LH 21006 (*contra* Cambra-Moo et al., 2006) and these range in morphology from plump to flat; the presence of vascular channels in these specimens may have obviated the need for the larger size class of osteocyte lacunae. They are also not present in the *Parvavis* section (*contra* Wang et al., in press), which could be due to ontogeny (only present in adults) or potentially this feature is limited to a fairly exclusive lineage of Late Cretaceous enantiornithines.

The histological samples from *Concornis* LH 21006 and STM 29-8 are similar to the Late Cretaceous femora in that the thickest region of the compacta is the OCL (approximately 40%-45% the thickness of the compacta in *Concornis* LH 21006 and STM 29-8), characterized by parallel-fibered bone and interrupted by LAGs, as in PVL-4273 and MACN-S-01. However, in the Late Cretaceous sections the compacta is nearly entirely OCL; STM 29-8 and *Concornis* LH 21006 show a total of three distinct layers, with a more vascularized middle layer of

parallel fibered bone with primary and secondary osteons (Cambra-Moo et al., 2006). Because the middle layer is proportionately thinner in *Concornis* sp., the sample is significantly less vascularized compared to STM 29-8. In MACN-S-01 a tide line marks the boundary between the upper region and the ICL, as in STM 29-8 and *Concornis*; however, in MACN-S-01 this contact is very distinct, even, and the ICL it demarcates is much thinner (Chinsamy et al., 1995). The tide line observed in the humerus of STM 29-8 varies throughout the cross-section so that in some places the ICL approaches one-third the cortical thickness—similar variation is observed in the histological section from the tarsometatarsus of the Early Cretaceous *Concornis* LH 21006 (Cambra-Moo et al., 2006). An ICL is not present in the *Parvavis* holotype, which is formed entirely of avascular parallel-fibered bone with both plump and flat osteocyte lacunae loosely arranged in parallel.

The femoral section of STM 29-8, like the humeral section of *Jeholornis* STM 2-51, preserves a double LAG, not previously reported in any enantiornithine or Early Cretaceous bird, which correlates with an annulus and LAG in the humerus. Such double LAGs are occasionally observed in dinosaurs, including the controversial Late Cretaceous paravian *Rahonavis* (Chinsamy and Elzanowski, 2001; Chinsamy et al., 1998) and are frequently found in amphibians (Liao and Lu, 2010). The presence of a double or accessory LAG has been interpreted as indicative of a bi-annual growth cycle (Chinsamy-Turan, 2005). This may suggest that enantiornithine growth strategies were diverse, or that this individual experienced some sort of trauma (that caused growth to be interrupted) during its life. However given that this feature occurs at the transition between the middle layer of more rapidly formed bone and the OCL, as in *Jeholornis* STM 2-51 and *Rahonavis* (Chinsamy and Elzanowski, 2001), and correlates with an annulus and LAG in the humerus, it is more likely that this double LAG marks the onset of sexual maturity (Lee and Werning, 2008). Another LAG may have been present close to the periosteal surface in STM 2-51. Four and five LAGs are preserved in PVL-4273 and MACN-S-01, respectively (Chinsamy et al., 1995). *Concornis* LH 21006 preserves at least two LAGs (Cambra-Moo et al., 2006). No LAGs are present in the holotype of *Parvavis* (Wang et al., in press).

Differences in bone tissue morphology observed between samples most likely primarily reflects differences in ontogenetic stage, however it is impossible to determine with the limited data whether or not growth is also affected by lineage specific trends (here strongly considered likely). Histological analysis of the *Gobipteryx* embryo indicates early bone formation was rapid, while PVL-4273 and MACN-S-01 indicate a prolonged period of slow growth (Chinsamy et al., 1995; Chinsamy and Elzanowski, 2001). Enantiornithines PVL-4273 and MACN-S-01 are considered adults—the absence of vascularized fibrolamellar bone tissue like that present in the *Gobipteryx* embryo is inferred to be due to the resorption of the more rapidly formed bone (deposited during early ontogeny) during medullary expansion (Chinsamy and Elzanowski, 2001). Indeed this embryonic fibrolamellar tissue is not present in any sampled post-natal specimen. The histology of *Concornis* LH 21006 and Enantiornithes indet. STM 29-8 reveal

an intermediate period of moderate post-natal growth suggesting three distinct growth stages during enantiornithine ontogeny: rapid embryonic growth (fibrolamellar bone tissue), moderate juvenile growth (rapidly formed parallel-fibered bone), and slow subadult growth until skeletal maturity (avascular parallel-fibered bone with flat, organized osteocyte lacunae). A similar pattern is inferred for *Sapeornis* although in this larger and more basal taxon, post-natal growth is faster producing woven-textured bone (Gao et al., 2012). The decrease in growth rate from the formation of more vascular to avascular bone is inferred to occur when sexual maturity is achieved (but since LAGs are present in PVL-4273 and MACN-S-01, growth did not cease) (Chinsamy et al., 1995; Chinsamy and Elzanowski, 2001). The change in bone tissue from more vascular to avascular observed in *Concornis* sp. and STM 29-8 suggests these specimens had reached sexual maturity; the incomplete fusion of the proximal carpometacarpus and proximal tarsals to the tibia in STM 29-8 suggests this specimen has not yet reached skeletal maturity. This means that, unlike living birds, the presence of an ICL and OCL in enantiornithines cannot be used as indicators of skeletal maturity (Ponton et al., 2004). The lesser degree of vascularization and thicker OCL containing two LAGs observed in *Concornis* LH 21006 suggests this specimen was more mature than STM 29-8 at the time of death, which is confirmed by the presence of a fully fused tibiotarsus and proximal tarsometatarsus in this specimen (Cabra-Moo et al., 2006). Furthermore, although the Argentine specimens are isolated femora, associated tibiotarsi and tarsometatarsi of comparable size are fully fused (Chiappe, 1993). This suggests that enantiornithines may continue to grow considerably even after compound skeletal elements fuse, unlike slow growing neornithine birds in which the fusion of the compound bones, in particular the distal tarsals to the metatarsals, typically marks the cessation of growth (Turvey and Holdaway, 2005).

The histology of *Parvavis* IVPP V 18586 complicates this interpretation of a three phase growth strategy for Enantiornithes. Although interpreted as a relatively mature subadult (Wang et al., in press), an alternate view is that this specimen is younger than the subadult STM 29-8, as indicated by the absence of LAGs and an ICL. This is consistent with the absence of fusion of compound bone in the holotype of *Parvavis*, despite a trend towards greater amounts of fusion in Late Cretaceous taxa relative to Early Cretaceous enantiornithines (O'Connor, 2009). Without additional samples, it is unknown if *Parvavis* would later experience a period of more rapid growth and deposit more vascularized bone tissue as it neared sexual maturity, as observed in Early Cretaceous enantiornithines, or if Late Cretaceous enantiornithine simply lacked vascularization in their post-natal bone tissue, and grew differently from Early Cretaceous enantiornithines. Although the adult body size of STM 29-8 is not exactly known, we can infer that it was considerably smaller than that of the Late Cretaceous specimens — all known Early Cretaceous enantiornithines are much smaller than the two sampled Late Cretaceous femora. Without a complete skeletal or histological growth series for any Early Cretaceous enantiornithine, we cannot determine whether or not the more vascular region of bone in STM 29-8 would be eventually lost during bone remodeling, leaving only avascular

OCL as observed in Late Cretaceous enantiornithines. However, differences between Early and Late Cretaceous samples suggest Late Cretaceous taxa may have evolved their own unique growth strategy.

4.3 Growth Trends in Basal Birds

Compared to *Jeholornis*, enantiornithine STM 29-8 shows a lesser degree of vascularization. This fits with the predicted model of dinosaur growth proposed by Erickson et al. (2009) — the smaller size of the enantiornithines means slower growth and more avascular bone relative to *Archaeopteryx*. However, the bone tissue in STM 29-8 differs from the larger Late Cretaceous femora PVL-4273 and MACN-S-01 in that it is relatively more highly vascularized. This suggests that the relationship between adult body size and growth rates proposed by Erickson et al. (2009) may not have been strictly true within Enantiornithes. Erickson et al. (2009) proposed that fast growing bone was lost in the ancestral avian line, due to dwarfism, and was regained during avian evolution, as evidenced by the more rapidly formed bone observed in *Sapeornis* (larger than *Archaeopteryx*) and derived birds. However, contra what is expected, larger enantiornithines show evidence for more slowly formed bone whereas small enantiornithines preserve faster growing tissue. This is reflected in the degree of vascularization; for their body size, Erickson et al. (2009) would predict a greater degree of vascularization in Late Cretaceous enantiornithines, not less. This would mean the clade departed from the dinosaurian growth pattern, but not convergent with the rapid growth strategy evolved within Ornithuromorpha, evolving their own unique growth strategy. Similarly, despite its considerably smaller size, *Confuciusornis* is more vascularized than *Jeholornis* and *Sapeornis*, while the increase in vascularization observed in the latter taxon relative to *Archaeopteryx* is greater than expected based on its only slight increase in size (Gao et al., 2012) indicating that Early Cretaceous basal birds in fact have non-dinosaurian growth patterns (*contra* Erickson et al., 2009). The unique growth strategy observed in Enantiornithes may have co-evolved with (or evolved as a result of) their unique super precocial developmental strategy (Chinsamy and Elzanowski, 2001; O'Connor, 2009).

4.4 Medullary bone in Mesozoic birds

Medullary bone is unique to egg-laying female birds including the ostrich with its proportionately small egg, and has been reported in a specimen of *T. rex* (Schweitzer et al., 2005) as well as several other dinosaurs (Lee and Werning, 2008) and one pterosaur (Chinsamy et al., 2009). Recently, it has been identified in the basal pygostylian bird, *Confuciusornis* (Chinsamy et al., 2013). It forms in response to estrogen produced in the body during yolk deposition (vitellogenesis), and provides a source of calcium for eggshell production (Miller and Bowman, 1981; Schweitzer et al., 2005). The two Mesozoic birds sampled here preserve female reproductive soft-tissue structures (ovarian follicles) indicating they were reproductively active (Zheng et al., 2013). Although there exists skepticism regarding this

interpretation (Mayr and Manegold, 2013), there exists no plausible alternative interpretation nor strong counter argument (O'Connor et al., 2013) and so we consider these structures to be ovarian follicles. Although in some samples the preserved bone is good quality, no medullary bone is observed in either STM 2-51 or STM 29-8. Medullary bone is extremely vascularized and could have been easily destroyed by crushing, thus its absence may potentially be taphonomic and the results are inconclusive. The persistence of medullary bone varies among extant birds; its absence in a specimen may also indicate the female died before its formation, which would suggest the preserved ovarian follicles were not mature.

Acknowledgements We thank Zhang Shukang (IVPP) for helping to prepare the samples and Jessie Atterholt (UC Berkeley), Josef Stiegler (GWU), Greg Erickson (FSU), and Anusuya Chinsamy-Turan (UCT) for helpful discussions. This research was supported by the National Basic Research Program of China (973 Program, 2012CB821906), the National Natural Science Foundation of China (41172020) and the Chinese Academy of Sciences.

早白垩世两只鸟类雌性个体的骨组织学研究

邹晶梅¹ 王敏¹ 郑晓廷^{2,3} 王孝理² 周忠和¹

(1 中国科学院古脊椎动物与古人类研究所, 中国科学院脊椎动物演化与人类起源重点实验室 北京 100044)

(2 临沂大学地质与古生物研究所 山东临沂 276000)

(3 山东天宇自然博物馆 山东平邑 273300)

摘要: 对发现于早白垩世热河生物群的两个达到性成熟的热河鸟(*Jeholornis* sp.)和反鸟(*Enantiornithes* indet.)的雌性个体进行了骨组织学研究。结果表明, 在热河鸟和反鸟中, 个体达到性成熟的时间要早于骨骼成熟。新的骨组织切片显示出与以往报道不同的骨组织结构, 表明中生代鸟类的骨组织结构在个体发育过程中的变化比原有的认识更为复杂。与以前报道过的热河鸟的骨组织结构相比, 本文研究的雌性热河鸟的骨骼切片显示出更高的血管化程度, 网状和径向的管道同时存在。反鸟的骨组织结构与此前报道过的早白垩世的反鸟*Concornis*相似, 其骨壁主要是由平行纤维板骨组成, 骨骼的血管化程度要高于以往报道过的反鸟成年个体。骨组织结构显示出该反鸟个体的骨质沉积速率已明显下降, 表明其已经达到了性成熟阶段。

关键词: 中生代, 组织学, 热河鸟, 反鸟, 热河生物群

中图法分类号: Q915.865 **文献标识码:** A **文章编号:** 1000-3118(2014)01-0112-17

References

- Bennett M B, 2008. Post-hatching growth and development of the pectoral and pelvic limbs in the black noddy, *Anous minutus*. *Comp Biochem Phys A*, 150(2): 159-168

- Benton M J, Zhou Z H, Orr P J et al., 2008. The remarkable fossils from the Early Cretaceous Jehol biota of China and how they have changed our knowledge of Mesozoic life. *Proc Geol Assoc*, 119: 209–228
- Cambra-Moo O, Buscalioni A D, Cubo J et al., 2006. Histological observations of enantiornithine bone (Saurischia, Aves) from the Lower Cretaceous of Las Hoyas (Spain). *C R Palevol*, 5(3): 685–691
- Castanet J, Francillon-Viellet H, Meunier E J et al., 1993. Bone and individual aging. In: Hall B K ed. *Bone*. London: CRC Press. 245–283
- Chang M M, Chen P J, Wang Y Q et al., 2003. *The Jehol Fossils: The Emergence of Feathered Dinosaurs, Beaked Birds and Flowering Plants*. Shanghai: Shanghai Scientific & Technical Publishers. 1–209
- Chiappe L M, 1993. Enantiornithine (Aves) tarsometatarsi from the Cretaceous Lecho Formation of northwestern Argentina. *Am Mus Novit*, 3083: 1–27
- Chinsamy A, Chiappe L M, Dodson P, 1994. Growth rings in Mesozoic birds. *Nature*, 368: 196–197
- Chinsamy A, Chiappe L M, Dodson P, 1995. Mesozoic avian bone microstructure: physiological implications. *Paleobiology*, 21(4): 561–574
- Chinsamy A, Chiappe L M, Marugán-Lobón J et al., 2013. Gender identification of the Mesozoic bird *Confuciusornis sanctus*. *Nat Commun*, doi: 10.1038/ncomms2377
- Chinsamy A, Codorniu L, Chiappe L M, 2009. Palaeobiological implications of the bone histology of *Pterodaustro guinazui*. *Anat Rec*, 292(9): 1462–1477
- Chinsamy A, Elzanowski A, 2001. Evolution of growth pattern in birds. *Nature*, 412: 402–403
- Chinsamy A, Rich T, Vickers-Rich P, 1998. Polar dinosaur bone histology. *J Vert Paleont*, 18(2): 385–390
- Chinsamy-Turan A, 2005. *The Microstructure of Dinosaur Bone: Deciphering Biology with Fine-Scale Techniques*. Baltimore: The Johns Hopkins University Press. 1–216
- de Ricqlès A, 1976. Recherches paléohistologiques sur les os longs des tétrapodes VII. — Sur la classification, la signification fonctionnelle et l'histoire des tissus osseux de tétrapodes (deuxième partie). *Ann Paléont (Vertébr)*, 62(1): 71–126
- de Ricqlès A J, Padian K, Horner J R et al., 2003. Osteohistology of *Confuciusornis sanctus* (Theropoda: Aves). *J Vert Paleont*, 23(2): 373–386
- Erickson G M, Rauhut O W M, Zhou Z H et al., 2009. Was dinosaurian physiology inherited by birds? Reconciling slow growth in *Archaeopteryx*. *PLoS ONE*, 4(10): e7390
- Forster C A, Sampson S D, Chiappe L M et al., 1998. The theropod ancestry of birds: new evidence from the Late Cretaceous of Madagascar. *Science*, 279: 1915–1919
- Gao C L, Chiappe L M, Zhang F J et al., 2012. A subadult specimen of the Early Cretaceous bird *Sapeornis chaoyangensis* and a taxonomic reassessment of sapeornithids. *J Vert Paleont*, 32(5): 1103–1112
- Hou L H, Zhang J Y, 1993. A new fossil bird from Lower Cretaceous of Liaoning. *Vert PalAsiat*, 31(3): 217–224
- Lee A H, Werning S, 2008. Sexual maturity in growing dinosaurs does not fit reptilian growth models. *Proc Nat Acad Sci*, 105(2): 582–587
- Liao W B, Lu X, 2010. Age structure and body size of the Chuanxi Tree Frog *Hyla annectans chuanxiensis* from two different elevations in Sichuan (China). *Zool Anz*, 248: 255–263
- Liu D, Zhou Z H, Zhang Y G, 2012. Mass estimate and evolutionary trend in Chinese Mesozoic fossil birds. *Vert PalAsiat*, 50(1): 39–52
- Mayr G, Manegold A, 2013. Can ovarian follicles fossilize? *Nature*, 499: E1, doi:10.1038/nature12367

- Miller S C, Bowman B M, 1981. Medullary bone osteogenesis following estrogen administration to mature male Japanese quail. *Dev Biol*, 87(1): 52–63
- O'Connor J K, 2009. A systematic review of Enantiornithes (Aves: Ornithothoraces). Ph.D thesis. Los Angeles: Geological Sciences, University of Southern California. 1–600
- O'Connor J K, Chiappe L M, Bell A, 2011. Pre-modern birds: avian divergences in the Mesozoic. In: Dyke G D, Kaiser G eds. *Living Dinosaurs: the Evolutionary History of Birds*. New Jersey: J. Wiley & Sons. 39–114
- O'Connor J K, Zhou Z H, Zheng X T, 2013. Zheng et al. replying to G. Mayr & A. Manegold. *Nature*, 499: E1–E2, doi:10.1038/nature12368
- Ponton F, Elzanowski A, Castanet J et al., 2004. Variation of the outer circumferential layer in the limb bones of birds. *Acta Ornithol*, 39(2): 137–140
- Schweitzer M H, Wittmeyer J L, Horner J R, 2005. Gender-specific reproductive tissue in ratites and *Tyrannosaurus rex*. *Science*, 308: 1456–1460
- Turvey S T, Holdaway R N, 2005. Postnatal ontogeny, population structure, and extinction of the Giant Moa *Dinornis*. *J Morphol*, 265(1): 70–86
- Wang M, Zhou Z H, Xu G H (in press). The first enantiornithine bird from the Upper Cretaceous of China. *J Vert Paleont*
- Xu X, You H L, Kai D et al., 2011. An *Archaeopteryx*-like theropod from China and the origin of Avialae. *Nature*, 475: 465–475
- Zhang F C, Hou L H, Ouyang L, 1998. Osteological microstructure of *Confuciusornis*: preliminary report. *Vert Palasiat*, 36(2): 126–135
- Zheng X T, O'Connor J K, Huchzermeyer F W et al., 2013. Exceptional preservation of ovarian follicles in Early Cretaceous birds and implications for early evolution of avian reproductive behaviour. *Nature*, 495: 507–511
- Zhou Z H, 1995. Discovery of a new enantiornithine bird from the Early Cretaceous of Liaoning, China. *Vert Palasiat*, 33(2): 99–113
- Zhou Z H, 2004. The origin and early evolution of birds: discoveries, disputes, and perspectives from fossil evidence. *Naturwissenschaften*, 91: 455–471
- Zhou Z H, Barrett P M, Hilton J, 2003. An exceptionally preserved Lower Cretaceous ecosystem. *Nature*, 421: 807–814
- Zhou Z H, Jin F, Zhang J Y, 1992. Preliminary report on a Mesozoic bird from Liaoning, China. *Chin Sci Bull*, 37(16): 1365–1368
- Zhou Z H, Zhang F C, 2002. Largest bird from the Early Cretaceous and its implications for the earliest avian ecological diversification. *Naturwissenschaften*, 89: 34–38
- Zhou Z H, Zhang F C, 2006. Mesozoic birds of China — a synoptic review. *Vert Palasiat*, 44(1): 74–98